

Microwave Refractive Index Structure Constants Derived from Site Test Interferometer Data

PI: David D. Morabito (332H), Co-I's Longtao Wu (398K) & David P. Heckman (332H)
Program: Spontaneous Concept

Background:

Site Test Interferometers (STIs) have been deployed at the three Deep Space Network (DSN) tracking sites at Goldstone, California; Madrid, Spain; and Canberra, Australia. In addition, a STI has been deployed at the Kennedy Space Center in Florida. These instruments continuously monitor signals emitted by geostationary satellites. The STIs have been operating near-continuously for several years producing a comprehensive statistical database for reliable characterization of the sites.

The long-term statistics of the interferometer phase fluctuations are useful in characterizing a site for potential arraying applications as well as allowing site inter-comparisons under differing climatic conditions. The statistics vary among sites due to climate and altitude, and at any one site diurnally, seasonally, and with passage of weather systems. Previous work focused on characterizing the statistics of the phase delay fluctuations [1-3].

Project Objective:

The objective of this study is to revisit the multi-year STI data set for the Goldstone, Madrid and Canberra DSN sites as well as the KSC site, and derive estimates of the microwave refractive index structure constants (C_n^2) from which one can allow for a standard inter-comparison of weather effects on potential arrays at the different sites. In addition, the findings also reveal differences in the structure constants between STIs residing in the same site (seasonal and year-to-year).

Wet refractive index structure constants, C_n^2 , estimated from the STI phase delay data provide statistical measures of atmospheric turbulence and insight into the vertical height of the atmosphere.

Such information is useful for characterizing sites for conducting communications through the atmospheric channel. This is important for radio links at microwave frequencies where the atmospheric effects are more significant.

The statistics of the structure constant, C_n^2 , allow for characterization of atmospheric turbulence for a variety of climates: Goldstone (high desert), Madrid and Canberra (temperate), and KSC (subtropical).

Benefits to NASA and JPL (or significance of results):

The path-averaged C_n^2 can be used in the link design of future arrays used for K-band (26 GHz, 32 GHz) communications (useful for characterizing expected system performance), as well as provide contributions to atmospheric science.

The addition of this data type to weather analysis and forecasting tools provides for potential enhanced data return making use of weather forecasting for link design of upcoming tracks.

This will allow for enabling of missions that make use of higher RF frequency and optical communications that are more susceptible to weather effects.

FY 18/19 Results:

We generate the structure function from STI phase data.

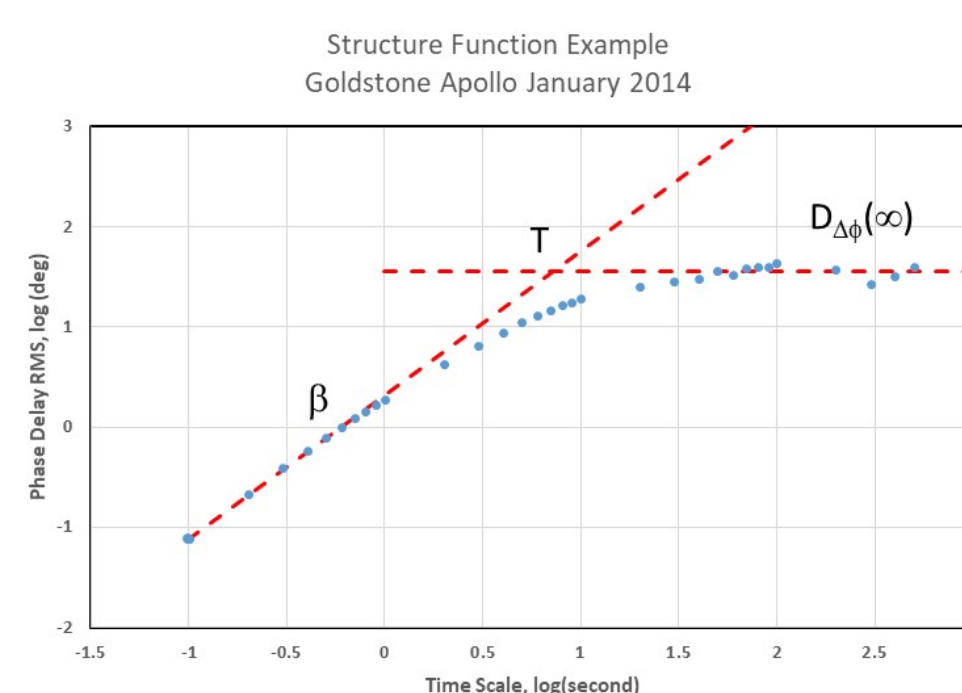


Table 1. Summary of experiment parameters at each measurement site.

Parameter	Goldstone, CA	Canberra, AUST	Madrid, Spain	KSC Florida
Latitude	35.340 N	35.2 S	40.24 N	28.51 N
Longitude	243.126 E	148.98 E	355.75 E	279.37 E
Altitude	964 m	690 m	830 m	3 m
Baseline Separation(s)	190 m	250 m	246 m	191 m
Elevation Angle	47.1°	48.2°	41.3°	55.6°
Frequency	12.45 GHz	11.95 GHz	11.95 GHz	12.45 GHz
Satellite	CIEL 2	OPTUS D3	EUTELSAT 9A	NIMIQ 5
Orbital Position	-129° E	156.1° E	9.0° E	287.3° E

From [1]

The refractive index structure constants can be estimated from the structure functions using formulation derived in the literature [4]:

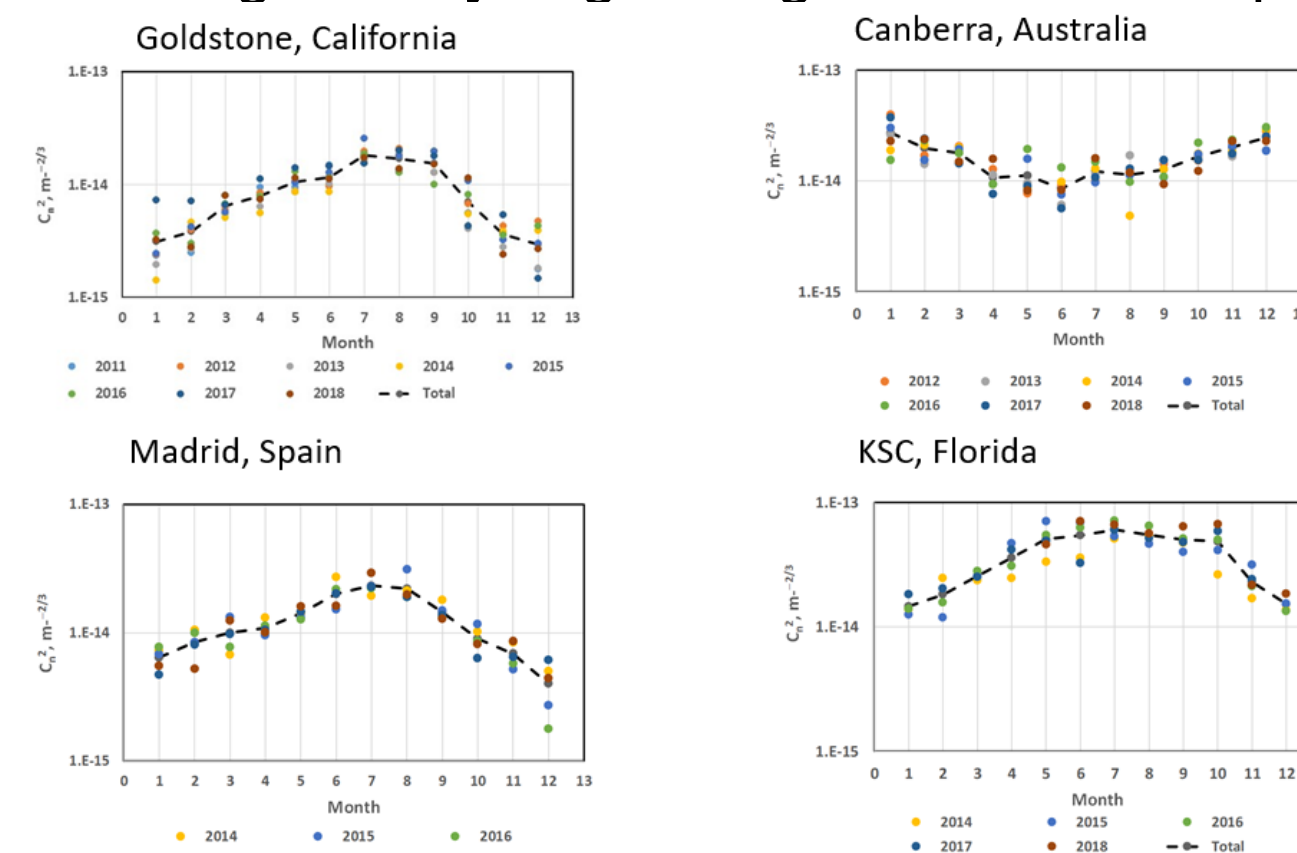
$$C_n^2 = \frac{D_{\Delta H}(\infty)}{5.82 d \beta_H}$$

where H is the effective height of the turbulent layer (m), β is the structure function slope at small time scales, $D_{\Delta H}(\infty)$ is the saturated path length variance (m^2), and d is the effective baseline length perpendicular to the signal path (m). $D_{\Delta H}(\infty)$ is calculated from phase variance $D_{\Delta \phi}(\infty)$ appropriately.

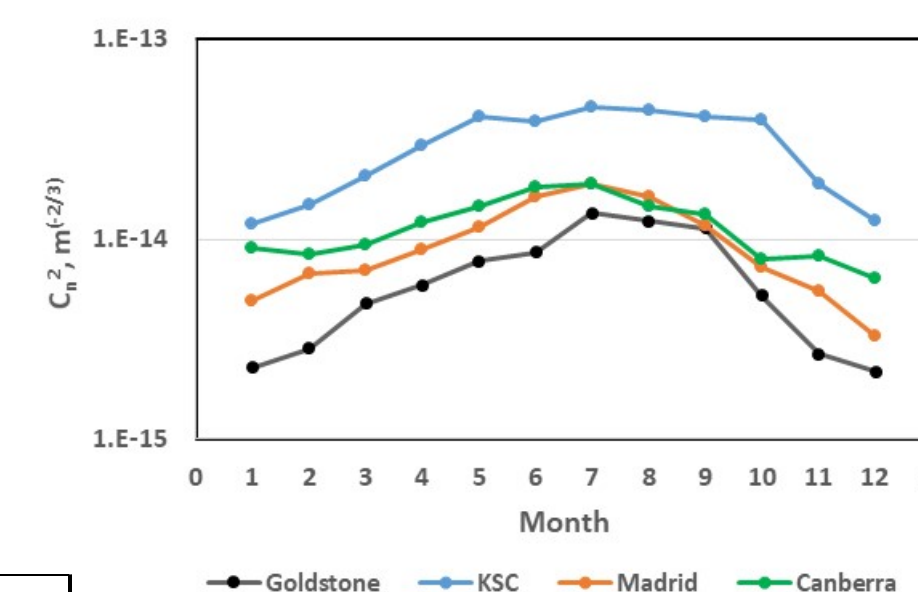
The results are shown below for the four STI sites with season (monthly averages) for the several year periods.

As expected, the high-desert Goldstone site shows the lowest values of C_n^2 , while the sub-tropical KSC site shows the highest values of C_n^2 . The two temperate climate sites of Madrid and Canberra fall in between.

These results are generally in good agreement with "spot checks" of C_n^2 from the literature [4-8].



Overall Average C_n^2 for each site vs. month (Adjusted to zenith for fair comparison; Canberra results offset by 6 months to align with seasons of north hemisphere STI sites)

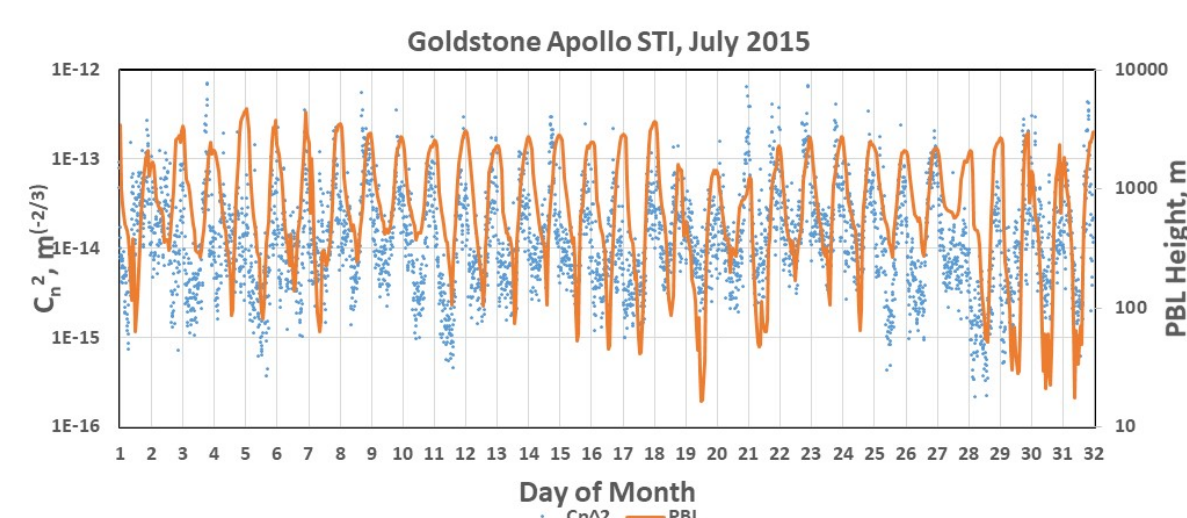


Instrument Site	Climate	Years of Data Collected	Overall Year		Summer Day		Winter Day		Summer Night		Winter Night	
			Average	Std. Dev	Average	Std. Dev	Average	Std. Dev	Average	Std. Dev	Average	Std. Dev
Goldstone	High Desert	2011-2018	6.62	4.05	23.07	4.94	2.85	1.40	5.42	5.27	2.12	1.40
Canberra	Temperate	2012-2018	11.92	4.40	27.47	6.72	12.45	4.79	8.36	6.72	7.72	4.79
Madrid	Temperate	2014-2018	9.76	4.92	40.22	8.47	4.16	1.87	5.97	8.47	2.84	1.87
KSC	Sub-Tropical	2014-2018	30.77	14.37	71.62	15.49	16.42	2.90	24.52	10.38	9.19	2.64

Plot at right of C_n^2 and Planetary Boundary Layer (PBL) height for Goldstone during July 2015 shows

Large day/night excursions
High degree of correlation
Correlation of PBL and C_n^2 not as significant at other sites.
Multiple linear analysis of C_n^2 with humidity (vapor pressure), temperature and PBL height to be reported on elsewhere (publication in preparation).

PBL extracted from the European Centre for Medium-Range Weather Forecasts (ECMWF) Re-Analysis Interim (ERA-Interim) data [9].



References:

- [1] David D. Morabito. Monthly and Annual Phase Delay Statistics Acquired from DSN and KSC Site Test Interferometers. The Interplanetary Network Progress Report, Volume 42-217, pp. 1-13, May 15, 2019.
- [2] Morabito, D. D., L. D'Addario, and S. Finley (2016). A comparison of atmospheric effects on differential phase for a two-element antenna array and nearby site test interferometer, Radio Sci., 51, doi:10.1002/2015RS005763.
- [3] Morabito, D. D., L. R. D'Addario, R. J. Acosta, and J. A. Nessel (2013). Tropospheric delay statistics measured by two site test interferometers at Goldstone, California, Radio Sci., 48, doi:10.1002/2013RS005268
- [4] J. A. Nessel and R. M. Manning, "Derivation of Microwave Refractive Index Structure Constant C_n^2 of the Atmosphere From K-Band Interferometric Phase Measurements," in IEEE Transactions on Antennas and Propagation, vol. 62, no. 11, pp. 5590-5598, Nov. 2014. doi: 10.1109/TAP.2014.2347997
- [5] G. Lanyi. Determination of the Tropospheric Fluctuation Coefficients in VLBI Parameter Estimates. The Telecommunications and Mission Operations Progress Report, Volume 42-133, pp. 1-6, May 15, 1998. https://ipnpr.jpl.nasa.gov/progress_report/42-133/1331.pdf
- [6] C. J. Naudet, "Estimation of Tropospheric Fluctuations Using GPS Data," The Telecommunications and Data Acquisition Progress Report 42-126, April-June 1996, Jet Propulsion Laboratory, Pasadena, California, pp. 1-19, August 15, 1996. <http://tmo.jpl.nasa.gov/tmo/progressreport/42-126/126A.pdf>
- [7] M. van Iersel, D. Paulson, C. Wu, N. Ferlic, J. Rzasa, C. Davis, M. Walker, M. Bowden, J. Sychalsky, and F. Titus, "Measuring the turbulence profile in the lower atmospheric boundary layer," Appl. Opt. 58, 6934-6941 (2019).
- [8] S. J. Keihm. Water Vapor Radiometer Measurements of the Tropospheric Delay Fluctuations at Goldstone Over a Full Year. The Telecommunications and Data Acquisition Progress Report, Volume 42-122, pp. 1-11, August 15, 1995.
- [9] Dee DP, et al. (2011) The ERA-Interim reanalysis: Configuration and performance of the data assimilation system. Q. J. R. Meteorol. Soc. 137: 553-597, doi:10.1002/qj.828

Publications:

Morabito, D. D., Longtao Wu, and David Heckman, "Radio Refractive Index of Wet Atmosphere Estimated from Site Test Interferometer Data", (in preparation)

PI/Task Mgr. Contact Information:

818-354-2424

David.D.Morabito@jpl.nasa.gov